

Multi-altitude Multi-sensor Fusion Framework for AUV Exploration and Survey

Jie Li and Matthew Johnson-Roberson*
Electrical Engineering and Computer Science
Naval Architecture and Marine Engineering*
University of Michigan, Ann Arbor, MI 48109
{ljlijie, mattjr}@umich.edu

Abstract—In this paper, we propose a path planning framework for underwater exploration and rugosity estimation using Autonomous Underwater Vehicles (AUVs). **Rugosity**, a measure of variation in the height of a surface, is commonly used to characterize seafloor habitat. The goal of this work is to optimize the survey of an unknown area in order to efficiently estimate its rugosity. To this end, we propose a novel rugosity approximation on 3D voxel grids and a novel framework for using that approximation to adaptively plan AUV paths. The proposed method employs a heterogeneous set of sensors – multi-beam sonar and stereo cameras – whose varied resolution and range make them complimentary for this task. For broad-scale exploration, sonar is used to produce a coarse sense of the area’s structure. Fine-scale exploration is completed using the stereo cameras to refine the high-resolution estimate of rugosity. Results display the simulation of two scenarios on real structural data gathered with an AUV and diver held sensor. The first scenario explores the situation where no broad-scale information is available and the robot must explore the terrain optically. The second simulates the two-pass case and demonstrates our method’s ability to achieve high accuracy rugosity estimation faster than other survey planning approaches.

I. INTRODUCTION

Optical benthic surveys of the underwater environment have found great success through the use of Autonomous Underwater Vehicles (AUVs) [1]. AUVs have generated excellent high-resolution imagery for mapping, and the autonomy of the vehicles has led to increases in the volume, accuracy, and repeatability of surveys. However, several factors make optically surveying the benthos challenging: the footprint/aperture and effective range of underwater high resolution sensors is very limited relative to aerial and terrestrial equivalents; battery life of AUVs is finite, limiting bottom time; and communications with the surface can be slow and unreliable. These factors make AUVs an expensive resource for benthic survey. Consequently, using this resource in the most efficient manner possible will greatly decrease the time and cost of surveying areas of interest at high resolution.

AUVs typically employ pre-planned survey patterns and utilize different types of sensor data independently. One method of increasing the efficiency of underwater surveys is to integrate survey data taken at higher altitude using longer-range sensors, like sonar. To better exploit this long-range data, we can employ adaptive path planning that prioritizes the surveying of the areas of greatest interest with the highest resolution and most coverage. In this paper we focus on one specific

problem domain for benthic monitoring: surveys intended for biological assessment. We further refine this abstraction to look specifically at terrain complexity. Terrain complexity is frequently used as a proxy for biodiversity and in many assessments of biological processes on the benthos [2]. In this paper we present a technique for efficiently characterizing the terrain complexity of the seafloor by adaptively directing an AUV. We adopt the paradigm presented by Friedman et al., which defines a terrain complexity model that generates rugosity values over a 3D mesh [3]. The main contributions of our framework are:

1. we propose a novel computationally efficient rugosity approximation.
2. we make the use of coarse resolution information collected from high-level survey to allow the low-level survey focus on area of importance.
3. we make use of the 3D structural information to help improve the path planning efficiency.

While the proposed techniques could be used to optimize many survey goals, we limit the scope of this work to the characterization of the rugosity of an area as quickly and efficiently as possible using a benthic surveying AUV.

The paper is structured as follows: we will discuss some prior works on autonomous path planning for different scenarios in Section II. Then we will give an overview on how we make use of long-range data in lower altitude survey in Section III. Finally, we evaluate the algorithm’s efficiency in Section IV. Conclusions and a discussion of future work appears in Section V.

II. PRIOR WORK

The view and path planning literature relevant to the presented work can be categorized based upon the degree to which the technique has access to prior information for planning. There are a class of techniques known as Next Best View (NBV) planning [4] which assume no knowledge about the structure prior to observation. As sensor data is acquired, the vehicle or sensor is directed to move in a manner which will increase the understanding of the object or scene given all of the currently observed data. This work uses either a surface model or a volumetric representation to plan new potential views of the scene. Surface-based techniques fit parametric models to existing data to determine how new unoccluded

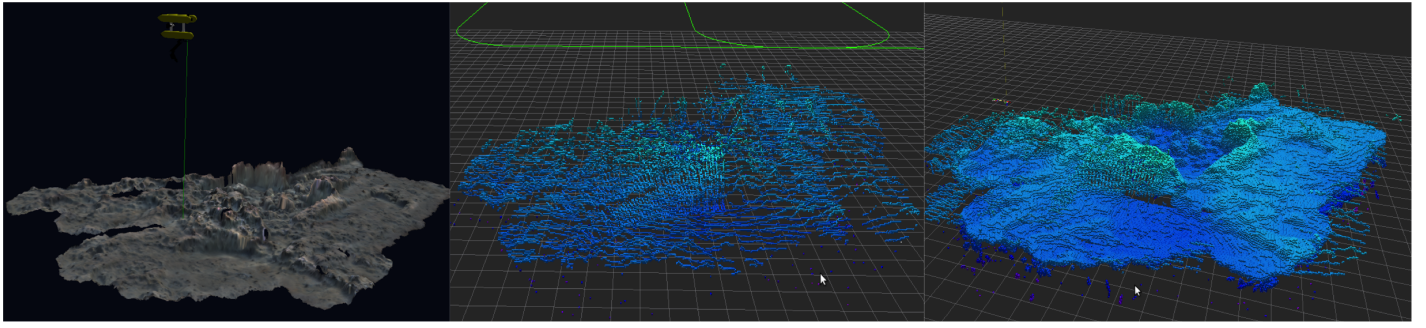


Figure 1. Terrain reconstruct reveals the rugosity information from a two-level AUV survey: In the high altitude survey, sensor resolution is low. We can collect a coarse structure of interesting areas. In the low altitude survey, the 3D structure model we estimated will be refined efficiently as the vehicle is performing our adaptive path.

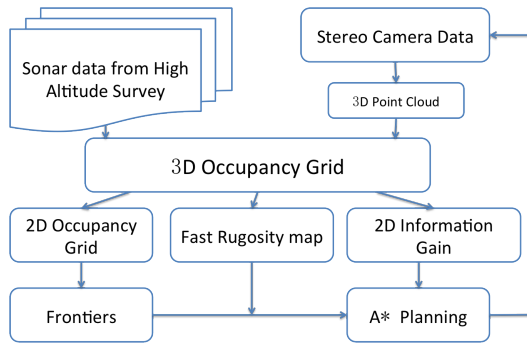


Figure 2. Framework pipeline – the exploration contains two levels of survey: 1) A high altitude survey using a sonar sensor is performed. The data from the sonar will be accumulated to initialize a coarse 3D occupancy map; 2) A low altitude survey is performed with an optical sensor. Several kinds of information will be extracted from a 3D occupancy map and used to adaptively plan a path.

views can be gathered [5]. Volumetric techniques subdivide the environment and reason about planning new views by examining voxel visibility given varying sensor locations and fields of view [4]. These techniques make strong use of the geometry of the vehicle and sensors, but are typically limited to small structures in indoor environments. In outdoor large scale surveys, Kim and Eustice apply NBV planning to maintain bounded error on a visual simultaneous localization and mapping (SLAM) system by modifying the vehicle’s path when localization error grows too large [6]. However, this work was not directly focused on optimizing a structural model. To some degree it achieves this by proxy through the generation of an accurate map and well localized set of features. Hollinger et al. propose a direct optimization of a 3D structural survey with an AUV by using a Gaussian Process (GP) to model a ship hull being surveyed [7]. This work does not incorporate prior observations. While the use of a GP enforces smoothness assumptions well suited to man-made objects, it is less relevant to the unstructured natural environments observed when performing biological survey. Galceran and Carreras propose a framework for planning coverage paths for ocean floor inspection [8]. They focus on generating practical coverage paths which follow constant-depth horizontal contours on the target surface. In contrast to the work we propose in this paper, their work is not directly

optimizing the information gain of the path.

For situations in which prior information exists, techniques often frame the problem from an information theoretic perspective. The largest body of work does this using a partially observable Markov decision process (POMDP). In this framework both the platform’s position and the sensor’s observations are uncertain. While this is a theoretically rigorous formulation of the problem, it becomes computationally intractable for large state spaces as it is PSPACE-complete [9]. This has led to many approximations of the generalized POMDP problem that allow for tractable solutions. Bender et al. use a GP to predict areas of the largest uncertainty to focus AUV dives for the greatest information gain. This work selects from a quiver of pre-planned dives and is focused on sampling. The space of possible trajectories required for 3D structural complexity surveys would render such a technique inapplicable [10]. Hollinger et al. implement an information gain optimizing sample based planner [11]. This technique also uses a GP for modeling the underlying process. It is focused on processes in 2D and as such its reward function does not lend itself to structural complexity mapping.

III. MULTI-ALTITUDE EXPLORATION

To achieve our goal of planning paths for AUVs to capture structural rugosity information more efficiently, we propose to combine two levels of exploration using different sensors. The flowchart of our proposed framework is shown in Figure 2. We model our knowledge of the space using a 3D occupancy grid. The high altitude survey will provide an initialization to the occupancy grid. In the adaptive path planning of low altitude exploration, structure information extracted from the 3D occupancy grid will be used within a costmap to optimize a path for the vehicle. The 3D occupancy grid will also be further updated using the observation from a low altitude survey. We will describe space modeling in greater detail in Section III-A, then discuss high altitude surveying in Section III-B. More details will be discussed on how we extract information from the 3D occupancy grid and how we perform the path planning using the extracted information in Section III-C.

A. Space Modeling

As shown in Figure 2, we use a 3D occupancy grid to represent our knowledge of the world based upon sensor observations. Hornung et al. implement a sparse 3D occupancy grid which we utilize here [12]. A 3D occupancy grid divides the space into voxels. An occupancy probability $P(n|z_{1:t})$ will be assigned each voxel as a measurement of observation uncertainty on the occupancy status of that cell.

Each voxel will be labeled as occupied, known (observed but not necessarily occupied), or free based on its occupancy probability. The occupancy probability is updated by the formula:

$$P(n|z_{1:t}) = [1 - \frac{1-P(n|z_t)}{P(n|z_t)} \frac{1-P(n|z_{1:t-1})}{P(n|z_{1:t-1})} \frac{1-P(n)}{P(n)}]^{-1}$$

Given the current measurement z_t , the occupancy probability $P(n|z_{1:t})$ is updated from the previous estimate $P(n|z_{1:t-1})$. $P(n)$ is uniformly initialized to a probability of 0.5 for every unseen node. This 3D grid will later be used to extract information about the scene in order to plan a path.

In the following section, we will introduce how we obtain a coarse 3D occupancy grid from a high altitude acoustic survey, which will help to prioritize a low altitude survey.

B. High altitude exploration

The first pass of the multi-altitude mapping is performed with an acoustic sensor at a range where optical mapping would be inapplicable (typically > 4 m dependent on water clarity). Acoustic sensors are commonly employed to perform benthic mapping. Sound propagates well through water enabling long range sensing. In this work we examine the use of a multi-beam sonar which is capable of quickly providing a broad-scale high-altitude map of the environment by making several high pass sweeps of an area. The downside of acoustic mapping is the lack of spatial resolution leading to the limited ability to characterize fine-scale rugosity. We employ a static complete coverage plan to get an overview of the area. Specifically, we use a Zamboni pattern, which is employed for vehicles with limited turning radii. An example is given in Figure 3. Note that the choice of path for high altitude survey is not critical assuming that it generates broad coverage of the area sufficient to seed the next steps of exploration. The data collected by the sonar sensor during the survey will be inserted into the occupancy grid. This coarse structural information will be used to direct the path planning as described in the following section.

C. Low altitude exploration

Low altitude exploration is done using active path planning based on the 3D occupancy grid described in the previous section. To determine the vehicle's path, we generate several possible short term goals, evaluate the priorities of these goals and establish a metric to search for an optimal path to the best goal with respect to estimating rugosity efficiently. The whole path planning strategy utilizes three different abstractions adaptively generated from the 3D occupancy grid: a 2D

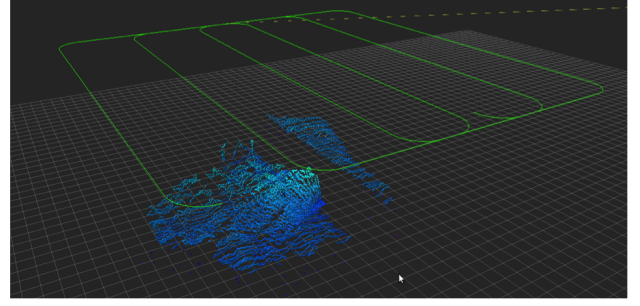


Figure 3. High altitude exploration with static path: High altitude survey is performed with a 'Zamboni' path, which will cover an area by a vehicle with a large turning radius. The data collected in this stage will be used to initialize an occupancy grid for a low altitude survey.

occupancy map, a fast rugosity map and a 2D information gain map. As shown in Figure 2, as the survey goes on, the stereo camera will observe the terrain and estimate a point cloud of the structure using dense stereo image processing. The point cloud will update the 3D occupancy grid to incorporate the most recent observations into each planning step. The three abstractions are presented below.

2D occupancy grid: The 2D occupancy grid represents the occupancy status of the XY plane when the vehicle is looking down. This is a 2D version of the 3D occupancy grid that facilitates efficient 2D lattice-based planning. We extract this by taking the maximum occupancy probability of all voxels in a Z-axis column. We also designate regions where the entire Z column has been observed and no longer requires exploration. This map gives us an overview of the geometric relationship between unknown and known area, which can be used to determine where the next candidate goal locations lie.

Fast rugosity map: The fast rugosity map is a grid-based representation of the structural rugosity of each location in the XY-plane. The definition of rugosity is the ratio between the actual length (or area) along the undulating terrain and the straight-line distance (or planar projected area). This is a compact expression of terrain complexity. As shown in Figure 4, when we observe a target with fixed resolution, the area with higher rugosity receives a lower spatial sampling rate than areas with lower rugosity. We propose that higher priority should be given to high rugosity areas to ensure uniform spatial sampling when imaging from overhead. This is done using the rugosity map to calculate the priority of possible goal locations.

Fine rugosity estimation is computationally expensive for a real-time planning system. To mitigate this we propose a fast rugosity approximation, as we are only interested in the relative relationship among different locations.

To speed up the rugosity calculation, the approximation makes use of the grid of cells instead of considering the full 3D structure of a mesh. We formulate this as:

$$R_{xy} = \frac{1}{N_{xy}} \sum_{\langle u,v \rangle \in C_{xy}} r_{uv} \cdot \mathbb{1}_{\{p_{uv} \text{ is occupied}\}}$$

$$r_{p_{uv}} = \frac{\|\overrightarrow{p_{uv}p_{(u+dx)v}} \times \overrightarrow{p_{uv}p_{u(v+dy)}}\|}{dx \cdot dy}$$

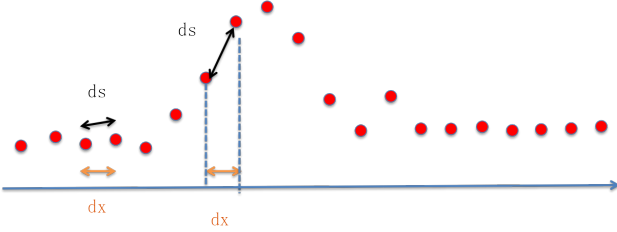


Figure 4. Rugosity and sampling rate: Here is a toy example considering only one dimension. Since the sensor is looking down, we assume an average sample rate on the horizontal axis. However, since the terrain has different rugosity, sampling distance on the terrain plane (or axis) is quite different. This indicates that the area with larger rugosity will end up with the lower sample rate, which results in higher information loss.

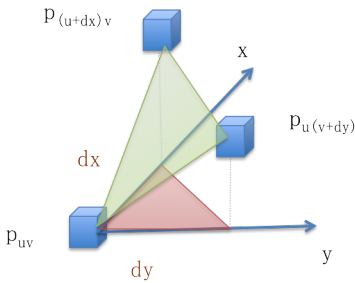


Figure 5. Fast rugosity approximation: a unit face to calculate the fast rugosity estimate is shown. The three points are 3D voxels in an occupancy grid with neighboring XY-coordinates. We use the ratio of the green area to the red area to approximate the rugosity at point P_{uv} . The method to calculate this ratio is discussed in

R_{xy} is the rugosity of a support area C_{xy} centered at location (x,y) . p_{uv} is the highest 3D point at location (u,v) . dx and dy are resolutions of the 3D occupancy grid. N_{xy} is the number of occupied p_{uv} in C_{xy} . A diagram with a toy example is shown in Figure 5. Fast rugosity at a single point is approximated by the ratio between the area of the unit surface (green face) and the projection area (red face).

The fast rugosity is just a rough approximation of terrain rugosity. However, our goal is to assign priority to potential paths based upon rugosity. The proposed approximation is sufficient for our application since it maintains the relative relationship of rugosity between different map locations regardless of the absolute error.

2D information gain: The 2D information gain map is a measurement of how much information the sensor could potentially obtain at a certain location. We first consider the information gain by observing any single voxels in the space. We treat the occupancy of a voxel as a Boolean random variable. Then the entropy of this random variable is:

$$H = -p \log p - (1-p) \log(1-p)$$

Each unknown voxel has a maximum entropy of $\log(2)$. When it's observed, the entropy will drop. The minimum entropy is reached when we are certain about whether it's occupied or free ($P=1/0$). So the maximum information we can obtain by observing a voxel is equals to its entropy. Considering a location at the vehicle's survey altitude, the information gain of one location is the sum of entropy of all voxels it can

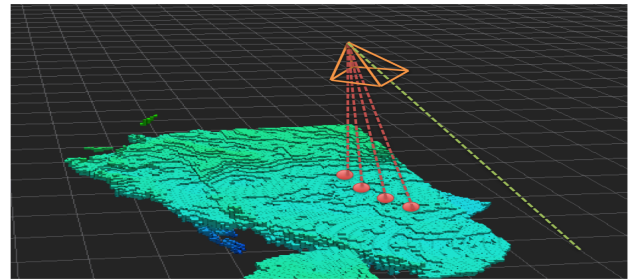


Figure 6. Information gain of camera : We cast sample rays from the camera position. The red rays that hit a voxel in the occupancy grid will have an information gain according to the occupancy probability of that voxel. For the green rays that go through nothing, we assume maximum information gain to be conservative.

observe in that location: $G_i = \sum_{j \in B_i} H(p_j)$. B_i is the set of voxels that can be observed from position i . We estimate B_i by casting simulated rays from the observing location according to the camera's resolution and field of view. As shown in Figure 6. If a ray hits an observed voxel, then the entropy of that voxel is added to the sum. If the ray does not hit any voxels, that indicates a location we have not explored. We will assign max entropy ($p = 0.5$) to that ray. We found little difference with both full and half resolution for ray casting. Thus, half resolution is used in our implementation for the sake of efficiency.

Adaptive Path Planning: We perform adaptive path planning for a low altitude survey based on the abstractions discussed above. The 2D occupancy grid will give us the geometric relationship between occupied, unknown, and undesired areas. We detect the boundary among unknown and occupied areas as possible goal locations. These locations are referred to as 'frontiers' in [13]. Then we rank the frontiers by comparing the rugosity in these locations using the fast rugosity map. Finally, the A* algorithm is employed to generate the path from current vehicle location to the target frontier. The cost of a trajectory $F(a)$ is defined as a weighted combination of path length and information gain. $F(a) = \alpha * \text{Length}(a) - \beta * \sum_{i \in a} G_i$, where α and β are corresponding weights that reflect the trade off between path length and information gain. Intuitively, optimal paths will be the paths that capture the maximum information gain while minimizing the path length. The path will be recalculated within a certain update-period when the vehicle is moving to capture the most up-to-date environment information.

IV. EXPERIMENT AND DISCUSSION

To evaluate the efficiency and robustness of our algorithm, we perform a set of simulations on real data gathered with an optical survey AUV and a diver held sensor [1]. With simulation results we are able to analyze accuracy and efficiency with respect to the ground truth data, which would be difficult to obtain for these experiments. We evaluate the algorithm under two different scenarios: when a high altitude survey is available for system initialization and when no high altitude survey information is available. We evaluate the proposed algorithm's performance using two metrics: 1) accuracy of the

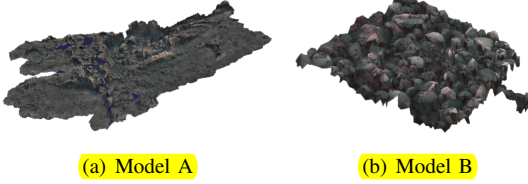


Figure 7. Terrain models used in the experiments

mesh surface reconstructed from the 3D occupancy grid, which evaluates how closely the sensed model matched the ground truth structure and 2) the accuracy of the rugosity estimation of the reconstructed mesh compared to that of the ground truth model.

In the following subsections we will first give more details on how we carry out the simulation then discuss the experimental results on different terrain models and different evaluation metrics.

A. Simulation Setting

We use a full 3D real time underwater simulator UWSim [14] to simulate the AUVs and underwater environment. UWSim is a powerful and popular underwater environment simulator for marine robotics research and development. For the input terrain model to UWSim, we use large-area dense coverage models gathered at high resolution and reconstructed using the previously published techniques of Johnson-Roberson et al. [15], [16]. These models have fine scale data across areas as large as $50 \times 75\text{ m}$. We include models of two different representative types of terrain to better evaluate the robustness of our framework. The models used in our experiment are shown in Figure 7. We evaluate our framework performance in the case where rugosity distribution is quite uneven (Model A) and also the case when rugosity is evenly distributed (Model B).

For virtual vehicles, we use Girona500 with a stereo camera set and a multi-beam sonar. The multi-beam Sonar used for the high-pass has a 60 degree swath width and an angular resolution of 0.1 degree. In the high altitude survey, the average distance from sonar sensor to terrain is 10 m in the high altitude survey. It leads to an average spacial resolution of 0.5 m on the benthos. In the low altitude survey, stereo cameras are used with the resolution of 1024×768 and a baseline of 0.12 m. The average distance from camera to terrain is 3 m in the low altitude survey.

B. Evaluation on Rugosity Estimation

The presented framework provide sufficient information for multi-scale terrain rugosity estimation [3]. Because of this, we expect our exploration strategy will decrease the error in dense rugosity estimation more efficiently than the other techniques. To evaluate this, we estimate terrain rugosity of mesh models constructed from 3D occupancy grids generated periodically over the course of the vehicle's exploration of the site, and compare them with the rugosity estimated from the ground truth model. Some details in the construction of the mesh model from the 3D occupancy grid will be given in IV-C.

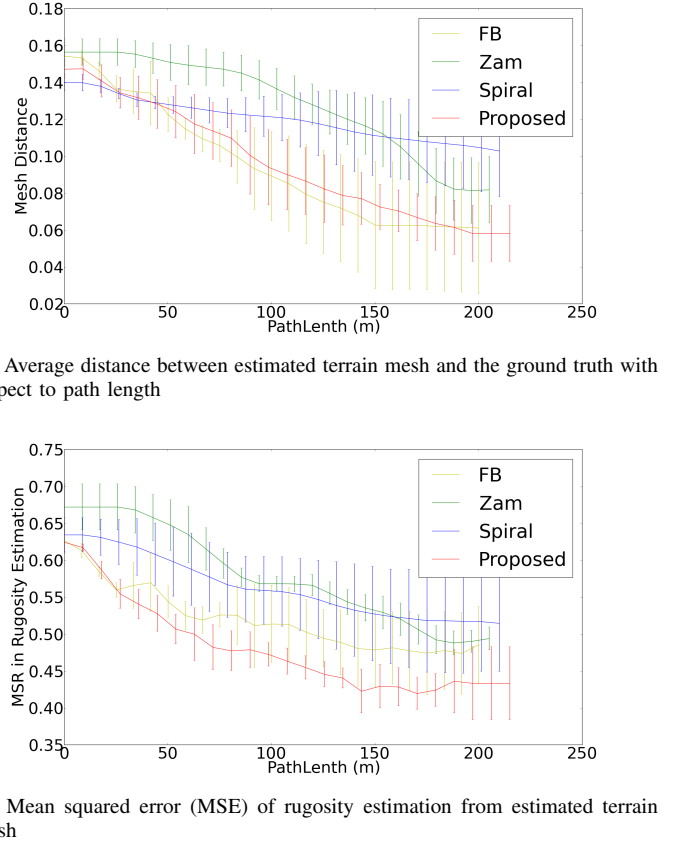


Figure 9. Results of surveys carried out on Terrain Model A with the high altitude survey as initial input.

Fig 9(b), 10(b), 11(b) and 12(b) show the difference in rugosity between the estimated model and the ground truth mesh model with respect to path length.

For underwater exploration, the global localization is challenging. The lack of the global positioning system (GPS) and the absence of clearly visible landmarks makes returning to a location on the benthos difficult. It is not uncommon to see 5-10 meters of error when returning to a target. To reflect this challenge we run a set of experiments with varying starting locations spaced 5m apart to realistically test the multi-level path planning problem under uncertain global pose. The error bar in the result figure shows the standard deviation of results from different starting locations.

Under all cases, both our method and the FB algorithm is more accurate and more consistent than static path planning, which is not surprising. It can be seen from Figure 9(b) and 11(b) that our proposed method always has a lower error in rugosity estimation when the high altitude observations are used. This result indicates the proposed method is more efficient in capturing the structural rugosity information than the other methods. By comparing the result from two different terrain models, we can tell that the benefit of the proposed method is greater when the rugosity is unevenly distributed. In the case when no high altitude information is available, as shown in Figure 10(b) and 12(b), our proposed method performs similarly to the FB algorithm.

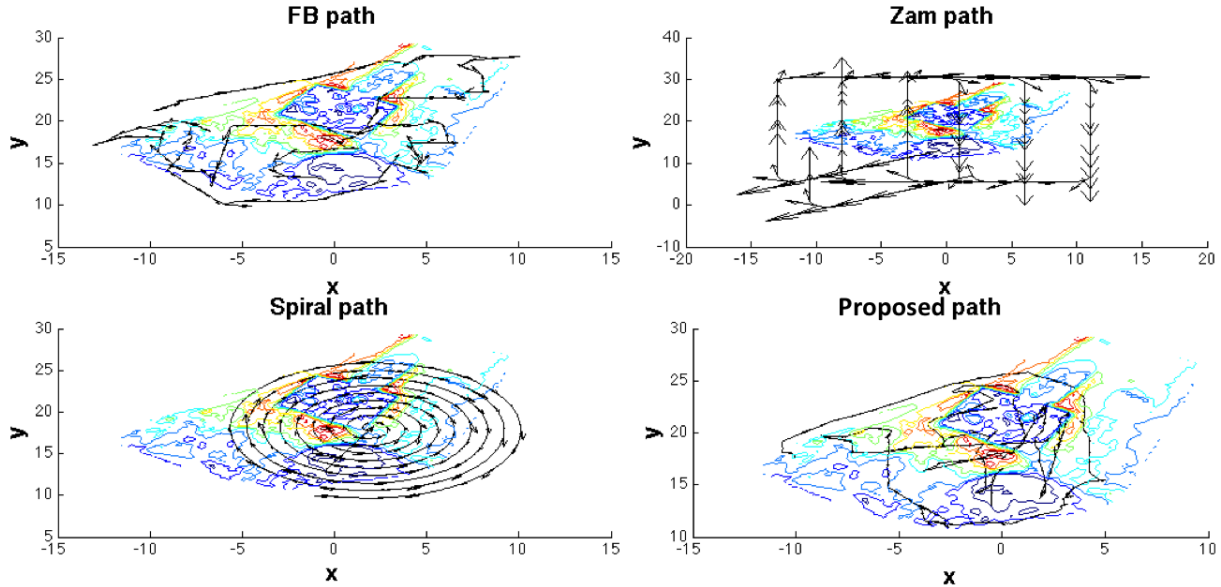
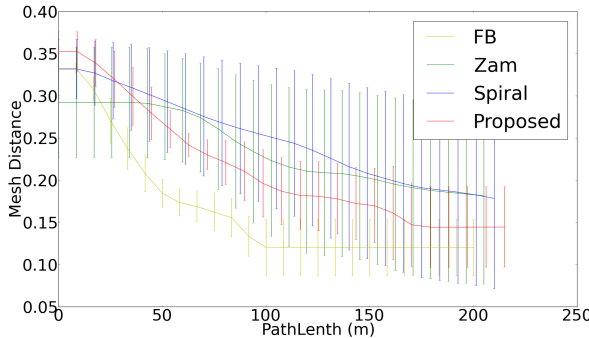
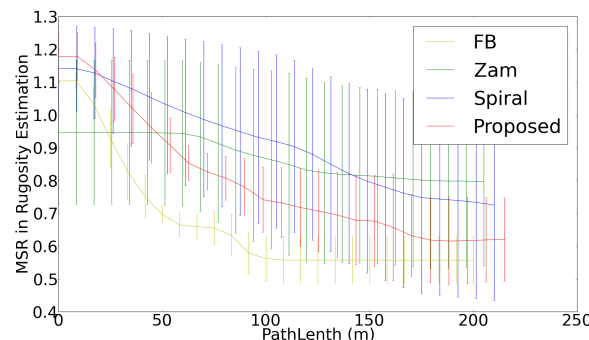


Figure 8. Typical path of the algorithm when exploring unknown areas: Path of 'Spiral', 'Zam', 'FB', 'Proposed method' are shown. The four algorithms have their paths shown overlaid on a contour map of the source data.



(a) Average distance between estimated terrain mesh and the ground truth with respect to path length



(b) Mean squared error (MSE) of rugosity estimation from estimated terrain mesh

Figure 9. Results of surveys carried out on Terrain Model A without the high altitude survey information

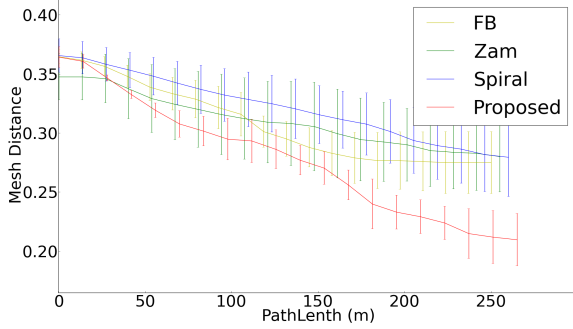
In the case when no high altitude survey has been performed, the trend of the error in rugosity estimation and mesh reconstruction is similar. The error is a function of the amount of area covered by the vehicle. However, when the data from the high altitude survey is used we note error is a function of coverage of the high relief areas. This can be attributed to the challenge of accurately capturing such areas from the high altitude survey. Additionally, the error in rugosity is more directly related to high relief area coverage than mesh error. The smoothness assumption in mesh reconstruction makes it a less sensitive error metric to data resolution.

The result indicates that our proposed method is able to provide a better rugosity estimation with the data from a high altitude survey as initial input.

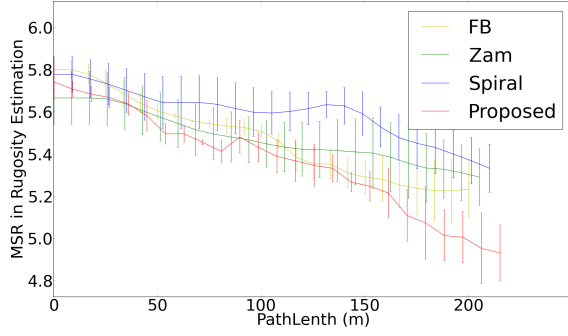
C. Evaluation on Mesh Reconstruction

Though our framework is targeted at rugosity estimation, structure reconstruction is an important output of any underwater visual survey. The accuracy of structure reconstruction is a key indicator to the quality of a survey for more general scenarios. In this experiment, we also consider the mesh reconstruction accuracy to evaluate our proposed method. We process the 3D occupancy grid into a mesh model and then compare it with the ground truth model. We take the center point of each voxel to form a 3D point cloud, then use Poisson Surface Reconstruction [17] to estimate a water tight surface mesh. We align the estimated mesh with the ground truth mesh model using Iterative Closest Point (ICP) [18]. Finally, the two meshes are compared by calculating the Hausdorff distance [19] between them. This gives us an error value expressing the similarity of the two models.

The error of the estimated mesh from the ground truth mesh model with respect to path length is shown. Figure 9(a), 10(a), 11(a) and 12(a) show the mean and standard



(a) Average distance between estimated terrain mesh and the ground truth with respect to path length



(b) Mean squared error (MSE) of rugosity estimation from estimated terrain mesh

Figure 11. Results of surveys carried out on Terrain Model B with the high level survey as initial input.

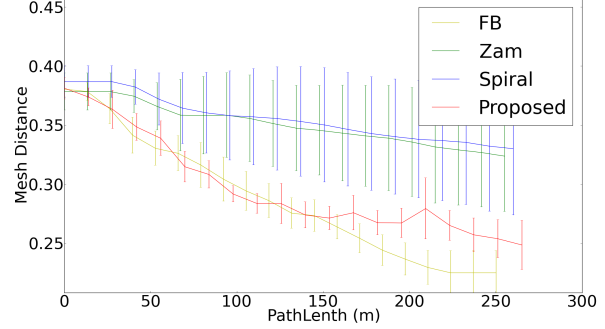
derivation of error for all experiments with different starting points.

In the case where the high altitude survey information is used, as shown in Figure 9(a) and 11(a), both the FB algorithm and proposed algorithm are more efficient than the static pattern path planners and less sensitive to the change in starting position. This can be attributed to the adaptive nature of these planning algorithms. Our proposed method performs similarly to the FB algorithm in terms of mesh reconstruction. This is expected, since we are not directly optimizing our path with respect to mesh reconstruction. In the case when the high altitude survey observations are used, the proposed algorithm tends to be more stable as shown by the error bar, as it takes global information into account. the FB algorithm is more sensitive to starting position in those cases since it performs frontier ranking based on local information.

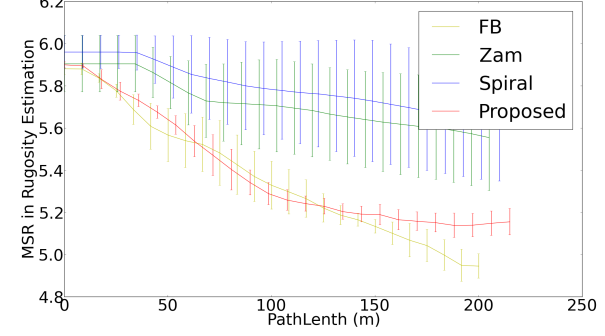
Our proposed method does not sacrifice efficiency in reconstructing the 3D structure when we target rugosity information. Is it also seen that our framework is able to utilize the high altitude survey to be more robust to starting position.

V. CONCLUSION

In this paper, we introduce a framework for path planning to explore an unknown area and estimate its rugosity. We achieve this by performing a high altitude survey using sonar prior to a low altitude survey using stereo cameras. We give



(a) Average distance between estimated terrain mesh and the ground truth with respect to path length



(b) Mean squared error (MSE) of rugosity estimation from estimated terrain mesh

Figure 12. Results of surveys carried out on Terrain Model B without the high level survey information

higher priority to high relief areas in the low altitude survey to optimize the information gain of the path. We evaluated our algorithm under a simulation using terrain data collected by real AUVs. Base-line methods are compared with our proposed framework to prove its robustness and efficiency. The results indicate that our algorithm performs more efficiently in capturing rugosity information of the structure while maintaining a high efficiency in structural reconstruction. For further exploration of this question, full 3D planning could be considered. Another avenue for future work would be building up an uncertainty model for the stereo camera that is corrected for water column effects.

REFERENCES

- [1] S. Williams, O. Pizarro, M. V. Jakuba, C. R. Johnson, N. S. Barrett, R. C. Babcock, G. A. Kendrick, P. D. Steinberg, A. J. Heyward, P. Doherty, I. Mahon, M. Johnson-Roberson, D. Steinberg, and A. Friedman, "Monitoring of benthic reference sites using an autonomous underwater vehicle," *IEEE Robotics and Automation Magazine*, vol. 19, no. 1, pp. 73–84, 2012.
- [2] M. I. McCormick, "Comparison of field methods for measuring surface topography and their associations with a tropical reef fish assemblage," *Marine ecology progress series. Oldendorf*, vol. 112, no. 1, pp. 87–96, 1994.
- [3] A. Friedman, O. Pizarro, S. B. Williams, and M. Johnson-Roberson, "Multi-scale measures of rugosity, slope and aspect from benthic stereo image reconstructions," *PLoS ONE*, vol. 7, p. e50440, 12 2012.
- [4] C. Connolly, "The determination of next best views," in *Robotics and Automation. Proceedings. 1985 IEEE International Conference on*, vol. 2, pp. 432–435, Mar 1985.

- [5] S. Chen and Y. Li, "Vision sensor planning for 3-d model acquisition," *Systems, Man, and Cybernetics, Part B: Cybernetics, IEEE Transactions on*, vol. 35, pp. 894–904, Oct 2005.
- [6] A. Kim and R. M. Eustice, "Next-best-view visual slam for bounded-error area coverage," in *IROS Workshop on Active Semantic Perception*, (Vilamoura, Portugal), October 2012.
- [7] G. A. Hollinger, B. Englert, F. Hover, U. Mitra, and G. S. Sukhatme, "Uncertainty-driven view planning for underwater inspection," in *Robotics and Automation (ICRA), 2012 IEEE International Conference on*, pp. 4884–4891, IEEE, 2012.
- [8] E. Galceran and M. Carreras, "Planning coverage paths on bathymetric maps for in-detail inspection of the ocean floor," in *Robotics and Automation (ICRA), 2013 IEEE International Conference on*, pp. 4159–4164, IEEE, 2013.
- [9] C. Papadimitriou and J. N. Tsitsiklis, "The complexity of markov decision processes," *Math. Oper. Res.*, vol. 12, pp. 441–450, Aug. 1987.
- [10] A. Bender, S. Williams, and O. Pizarro, "Autonomous exploration of large-scale benthic environments," in *Robotics and Automation (ICRA), 2013 IEEE International Conference on*, pp. 390–396, May 2013.
- [11] G. Hollinger and G. Sukhatme, "Sampling-based motion planning for robotic information gathering," in *Proceedings of Robotics: Science and Systems*, (Berlin, Germany), June 2013.
- [12] A. Hornung, K. M. Wurm, M. Bennewitz, C. Stachniss, and W. Burgard, "OctoMap: An efficient probabilistic 3D mapping framework based on octrees," *Autonomous Robots*, 2013.
- [13] B. Yamauchi, "A frontier-based approach for autonomous exploration," in *Computational Intelligence in Robotics and Automation, 1997. CIRA'97., Proceedings., 1997 IEEE International Symposium on*, pp. 146–151, Jul 1997.
- [14] M. Prats, J. Perez, J. Fernandez, and P. Sanz, "An open source tool for simulation and supervision of underwater intervention missions," *IEEE/RSJ International Conference on Intelligent Robots and Systems (IROS)*, pp. pp. 2577–2582, 7-12 Oct 2012.
- [15] M. Johnson-Roberson, O. Pizarro, S. B. Williams, and I. Mahon, "Generation and Visualization of Large-scale Three-dimensional Reconstructions from Underwater Robotic Surveys," *Journal of Field Robotics*, vol. 27, no. 1, pp. 21–51, 2010.
- [16] M. Johnson-Roberson, M. Bryson, B. Douillard, O. Pizarro, and S. B. Williams, "Out-of-core efficient blending for underwater georeferenced textured 3d maps," in *IEEE Computing for Geospatial Research and Application (COM. Geo), 2013 Fourth International Conference on*, pp. 8–15, 2013.
- [17] M. Kazhdan, M. Bolitho, and H. Hoppe, "Poisson surface reconstruction," in *Proceedings of the fourth Eurographics symposium on Geometry processing*, 2006.
- [18] Z. Zhang, "Iterative point matching for registration of free-form curves and surfaces," *International journal of computer vision*, vol. 13, no. 2, pp. 119–152, 1994.
- [19] M. Roy, S. Foufou, and F. Truchetet, "Mesh comparison using attribute deviation metric," *International Journal of Image and Graphics*, vol. 4, no. 01, pp. 127–140, 2004.